Shear Viscosity and Phase Diagram from Polyakov–Nambu–Jona-Lasinio model

Sudipa Upadhaya

Bose Institute

November 17, 2015

Based on :: PRD 91, 054005 (2015)

Prelude

Prelude

Ⓢ Expected transition for the exotic matter produced in the high-energy heavy-ion experiments.

Prelude

Ⓢ Expected transition for the exotic matter produced in the high-energy heavy-ion experiments.

Ⓢ Distinctive dynamic properties to be studied for signatures of such transitions, a quite gruelling stuff because of the short span existence of the so called Quark-Gluon Plasma (QGP).

Prelude

Ⓢ Expected transition for the exotic matter produced in the high-energy heavy-ion experiments.

Ⓢ Distinctive dynamic properties to be studied for signatures of such transitions, a quite gruelling stuff because of the short span existence of the so called Quark-Gluon Plasma (QGP).

Ⓢ Possibilities of studying transport properties of such deconfined state providing the opportunity to investigate the QCD phases like the cross-over, 1st order and the region of Critical End Point (CEP) expectedly a second order transition regime.

Prelude

♣ In hydrodynamical description, dissipative processes are quantified by the transport coefficients, shear (η) & bulk viscosity (ζ).

♣ Apart from carrying information on how far the system appears from ideality, their values and properties also provide relevant insight into the fluid's dynamics and its critical phenomena.

♣ For various materials e.g. Helium, Nitrogen or Water, specific shear viscosity $\frac{\eta}{s}$ is known experimentally to show a minimum at the phase transition. On the other hand, specific bulk viscosity $\frac{\zeta}{s}$ was argued to be maximum at that point.

♣ Henceforth, the bulk & shear viscosities near T_c modify the evolution of the QCD medium and influence phenomenological observables as well that characterise the expansion dynamics.

♣ Thus transport coefficients are of particular interest to quantify the properties of strongly interacting relativistic fluids and its phase transitions.

Reviewing some basics

Reviewing some basics

- The EoM of a viscous fluid may be obtained by adding to the ideal momentum flux a term σ'_{ik} which gives the irreversible viscous transfer of momentum in the fluid
  $\Pi_{ik} = p\delta_{ik} + \rho v_i v_k - \sigma'_{ik}$

Reviewing some basics

- The EoM of a viscous fluid may be obtained by adding to the ideal momentum flux a term σ'_{ik} which gives the irreversible viscous transfer of momentum in the fluid
  $\Pi_{ik} = p\delta_{ik} + \rho v_i v_k - \sigma'_{ik}$
  - Depends on space derivatives of the velocity.

Reviewing some basics

- The EoM of a viscous fluid may be obtained by adding to the ideal momentum flux a term σ'_{ik} which gives the irreversible viscous transfer of momentum in the fluid
  $\Pi_{ik} = p\delta_{ik} + \rho v_i v_k - \sigma'_{ik}$
  - Depends on space derivatives of the velocity.
  - Supposed to be a linear function of $\frac{\partial v_i}{\partial x_k}$.

Reviewing some basics

- The EoM of a viscous fluid may be obtained by adding to the ideal momentum flux a term σ'_{ik} which gives the irreversible viscous transfer of momentum in the fluid
  $\Pi_{ik} = p\delta_{ik} + \rho v_i v_k - \sigma'_{ik}$
  - Depends on space derivatives of the velocity.
  - Supposed to be a linear function of $\frac{\partial v_i}{\partial x_k}$.
  - Symmetrical combinations of the derivatives $\frac{\partial v_i}{\partial x_k}$.

Reviewing some basics

- The EoM of a viscous fluid may be obtained by adding to the ideal momentum flux a term σ'_{ik} which gives the irreversible viscous transfer of momentum in the fluid
  $\Pi_{ik} = p\delta_{ik} + \rho v_i v_k - \sigma'_{ik}$
  - Depends on space derivatives of the velocity.
  - Supposed to be a linear function of $\frac{\partial v_i}{\partial x_k}$.
  - Symmetrical combinations of the derivatives $\frac{\partial v_i}{\partial x_k}$.

$$\sigma'_{ik} = \eta\left(\frac{\partial v_i}{\partial x_k} + \frac{\partial v_k}{\partial x_i} - \frac{2}{3}\partial_{ik}\frac{\partial v_l}{\partial x_l}\right) + \zeta\delta_{ik}\frac{\partial v_l}{\partial x_l}$$

Kubo Formalism

- The Kubo formula for shear viscosity gives,

$$\eta(\omega) = \frac{1}{15T} \int_0^\infty dt e^{i\omega t} \int d\vec{r} (T_{\mu\nu}(\vec{r}, t), T_{\mu\nu}(0,0))$$

- The Kubo formula can also be rewritten as,

$$\eta(\omega) = \beta \int_0^\infty dt e^{i\omega t} \int d\vec{r} (T_{21}(\vec{r}, t), T_{21}(0,0)) = \frac{i}{\omega} [\Pi^R(\omega) - \Pi^R(0)]$$

with retarded correlator,

$$\Pi^R(\omega) = -i \int_0^\infty dt e^{i\omega t} \int d^3\vec{r} < [T_{21}(\vec{r}, t), T_{21}(0)] >$$

Continued

- To calculate the retarded correlator, we use Matsubara formalism

$$\Pi(\omega_n) = \frac{1}{\beta}\sum_l \int \frac{d^3p}{(2\pi)^3} p^2 Tr[\gamma_2 G(\vec{r},\omega_l+\omega_n)\gamma_2 G(\vec{p},\omega_l)]$$

This leads to,

$$\eta = \frac{\pi}{T}\int_{-\infty}^{\infty}\int \frac{d^3p}{(2\pi)^3} p^2 f_\Phi(1-f_\Phi) Tr[\gamma_2\rho(\epsilon,p)\gamma_2\rho(\epsilon,p)]$$

- On evaluating the trace we get,

$$\eta[\Gamma(p)] = \frac{16N_cN_f}{15\pi^3 T}\int_{-\infty}^{\infty}\int_0^{\infty} dpp^6 \frac{M^2\Gamma^2(p)f_\Phi(\epsilon)(1-f_\Phi(\epsilon))}{((\epsilon^2-p^2-M^2+\Gamma^2(p))^2+4M^2\Gamma^2(p))^2}$$

PNJL Model

PNJL Model

$\Leftrightarrow$ A QCD inspired phenomenological model developed by coupling the Polyakov loop potential to the old Nambu-Jona-Lasinio Model.

PNJL Model

$\Leftrightarrow$ A QCD inspired phenomenological model developed by coupling the Polyakov loop potential to the old Nambu-Jona-Lasinio Model.

$\Leftrightarrow$ In NJL model spontaneous breaking of chiral symmetry takes place due to the dynamical generation of fermionic mass.

PNJL Model

$\Leftrightarrow$ A QCD inspired phenomenological model developed by coupling the Polyakov loop potential to the old Nambu-Jona-Lasinio Model.

$\Leftrightarrow$ In NJL model spontaneous breaking of chiral symmetry takes place due to the dynamical generation of fermionic mass.

$\Leftrightarrow$ However, gluon dynamics being sucessfully incorporated by the background temporal field, PNJL model encapsulates the deconfinement physics as well. The chiral and deconfinement order parameters are entwined into a single framework.

PNJL Model

$\Leftrightarrow$ A QCD inspired phenomenological model developed by coupling the Polyakov loop potential to the old Nambu-Jona-Lasinio Model.

$\Leftrightarrow$ In NJL model spontaneous breaking of chiral symmetry takes place due to the dynamical generation of fermionic mass.

$\Leftrightarrow$ However, gluon dynamics being sucessfully incorporated by the background temporal field, PNJL model encapsulates the deconfinement physics as well. The chiral and deconfinement order parameters are entwined into a single framework.

$\Leftrightarrow$ Henceforth, using the thermodynamic potential we can find the fields, pressure and constituent masses for corresponding T & μ.

PNJL model formalism[2]

[1] S.K.Ghosh,T.K.Mukherjee,M.G.Mustafa and R.Ray, PRD 77, 094024 (2008)
[2] S.K.Ghosh,T.K.Mukherjee,M.G.Mustafa and R.Ray, PRD 73, 114007 (2006)

PNJL model formalism[2]

- Thermodynamic potential for PNJL model

$$\Omega = \mathcal{U}'[\Phi, \bar{\Phi}, T] + 2g_S(\sigma_u^2 \; + \; \sigma_d^2) \; - \; \frac{g_D}{2}\sigma_u\sigma_d\sigma_s + 3\frac{g_1}{2}(\sigma_f^2)^2 + 3g_2\sigma_f^4 - 6\sum_{f=u,d}\int_0^\Lambda \frac{d^3p}{(2\pi)^3} E_f\Theta(\Lambda - |\vec{p}|)$$
$$- 2T\sum_{f=u,d}\int_0^\infty \frac{d^3p}{(2\pi)^3}\ln\left[1 + 3(\Phi + \bar{\Phi}e^{-\frac{(E_f-\mu_f)}{T}})e^{-\frac{(E_f-\mu_f)}{T}} + e^{-3\frac{(E_f-\mu_f)}{T}}\right]$$
$$- 2T\sum_{f=u,d}\int_0^\infty \frac{d^3p}{(2\pi)^3}\ln\left[1 + 3(\bar{\Phi} + \Phi e^{-\frac{(E_f+\mu_f)}{T}})e^{-\frac{(E_f+\mu_f)}{T}} + e^{-3\frac{(E_f+\mu_f)}{T}}\right]$$

[1] S.K.Ghosh,T.K.Mukherjee,M.G.Mustafa and R.Ray, PRD 77, 094024 (2008)
[2] S.K.Ghosh,T.K.Mukherjee,M.G.Mustafa and R.Ray, PRD 73, 114007 (2006)

PNJL model formalism[2]

- Thermodynamic potential for PNJL model

$$\Omega = \mathcal{U}'[\Phi, \bar{\Phi}, T] + 2g_S(\sigma_u^2 + \sigma_d^2) - \frac{g_D}{2}\sigma_u\sigma_d\sigma_s + 3\frac{g_1}{2}(\sigma_f^2)^2 + 3g_2\sigma_f^4 - 6\sum_{f=u,d}\int_0^\Lambda \frac{d^3p}{(2\pi)^3} E_f \Theta(\Lambda - |\vec{p}|)$$
$$- 2T\sum_{f=u,d}\int_0^\infty \frac{d^3p}{(2\pi)^3} \ln\left[1 + 3(\Phi + \bar{\Phi}e^{-\frac{(E_f-\mu_f)}{T}})e^{-\frac{(E_f-\mu_f)}{T}} + e^{-3\frac{(E_f-\mu_f)}{T}}\right]$$
$$- 2T\sum_{f=u,d}\int_0^\infty \frac{d^3p}{(2\pi)^3} \ln\left[1 + 3(\bar{\Phi} + \Phi e^{-\frac{(E_f+\mu_f)}{T}})e^{-\frac{(E_f+\mu_f)}{T}} + e^{-3\frac{(E_f+\mu_f)}{T}}\right]$$

- where the P-loop potential[1],

$$\frac{\mathcal{U}'(\Phi,\bar{\Phi},T)}{T^4} = \frac{\mathcal{U}(\Phi,\bar{\Phi},T)}{T^4} - \kappa ln[J(\phi,\bar{\phi})]$$

[1] S.K.Ghosh,T.K.Mukherjee,M.G.Mustafa and R.Ray, PRD 77, 094024 (2008)
[2] S.K.Ghosh,T.K.Mukherjee,M.G.Mustafa and R.Ray, PRD 73, 114007 (2006)

Contd.

Contd.

- $\mathcal{U}(\Phi)$ is the Landau-Ginzburg potential given by,
  $\frac{\mathcal{U}(\Phi,\bar{\Phi},T)}{T^4} = -\frac{b_2(T)}{2}\bar{\Phi}\Phi - \frac{b_3}{6}\left(\Phi^3 + \bar{\Phi}^3\right) + \frac{b_4}{4}\left(\bar{\Phi}\Phi\right)^2$
  with, $b_2(T) \;=\; a_0 \;+\; a_1\left(\frac{T_0}{T}\right) \;+\; a_2\left(\frac{T_0}{T}\right)^2 \;+\; a_3\left(\frac{T_0}{T}\right)^3$

Contd.

- $\mathcal{U}(\Phi)$ is the Landau-Ginzburg potential given by,
  $\frac{\mathcal{U}(\Phi,\bar{\Phi},T)}{T^4} = -\frac{b_2(T)}{2}\bar{\Phi}\Phi - \frac{b_3}{6}\left(\Phi^3 + \bar{\Phi}^3\right) + \frac{b_4}{4}\left(\bar{\Phi}\Phi\right)^2$
  with, $b_2(T) \;=\; a_0 \;+\; a_1\left(\frac{T_0}{T}\right) \;+\; a_2\left(\frac{T_0}{T}\right)^2 \;+\; a_3\left(\frac{T_0}{T}\right)^3$

- First job is to minimise Ω and get the field values. Equations to be solved are: $\frac{\partial\Omega}{\partial\sigma_u} \;=\; 0$, $\frac{\partial\Omega}{\partial\sigma_d} \;=\; 0$, $\frac{\partial\Omega}{\partial\Phi} \;=\; 0$ & $\frac{\partial\Omega}{\partial\bar{\Phi}} \;=\; 0$

Contd.

- $\mathcal{U}(\Phi)$ is the Landau-Ginzburg potential given by,
  $\frac{\mathcal{U}(\Phi,\bar{\Phi},T)}{T^4} = -\frac{b_2(T)}{2}\bar{\Phi}\Phi - \frac{b_3}{6}\left(\Phi^3 + \bar{\Phi}^3\right) + \frac{b_4}{4}\left(\bar{\Phi}\Phi\right)^2$
  with, $b_2(T) \;=\; a_0 \;+\; a_1\left(\frac{T_0}{T}\right) \;+\; a_2\left(\frac{T_0}{T}\right)^2 \;+\; a_3\left(\frac{T_0}{T}\right)^3$

- First job is to minimise Ω and get the field values. Equations to be solved are: $\frac{\partial\Omega}{\partial\sigma_u} \;=\; 0\,,\; \frac{\partial\Omega}{\partial\sigma_d} \;=\; 0\,,\; \frac{\partial\Omega}{\partial\Phi} \;=\; 0$ & $\frac{\partial\Omega}{\partial\bar{\Phi}} \;=\; 0$

- The distribution functions for the particles and antiparticles are
  $f_{\Phi}^{+} = \frac{(\bar{\Phi}+2\Phi e^{-\beta(E_p+\mu)})e^{-\beta(E_p+\mu)}+e^{-3\beta(E_p+\mu)}}{1+3(\bar{\Phi}+\Phi e^{-\beta(E_p+\mu)})e^{-\beta(E_p+\mu)}+e^{-3\beta(E_p+\mu)}}$
  $f_{\Phi}^{-} = \frac{(\Phi+2\bar{\Phi} e^{-\beta(E_p-\mu)})e^{-\beta(E_p-\mu)}+e^{-3\beta(E_p-\mu)}}{1+3(\Phi+\bar{\Phi} e^{-\beta(E_p-\mu)})e^{-\beta(E_p-\mu)}+e^{-3\beta(E_p-\mu)}}$

Parametrization

Parametrization

$\Leftrightarrow$ Inspecting the detailed behavior of the integrand, we see that η converges for the criterion, $\eta[\Gamma(p)] < \infty \Leftrightarrow p^3 e^{-\beta p/2} \in o(\Gamma(p))$ where, o(-) denotes the Little-Landau symbol.

Parametrization

$\Leftrightarrow$ Inspecting the detailed behavior of the integrand, we see that η converges for the criterion, $\eta[\Gamma(p)] < \infty \Leftrightarrow p^3 e^{-\beta p/2} \in o(\Gamma(p))$ where, o(-) denotes the Little-Landau symbol. The feasible configurations of Γ satisfying the above conditions are ::

$$Constant : \Gamma_{constant} = 100 MeV$$

$$Exponential : \Gamma_{exp}(p) = \Gamma_{constant} e^{-\beta p/8}$$

$$Lorentzian : \Gamma_{Lor}(p) = \Gamma_{constant} \frac{\beta p}{1+(\beta p)^2}$$

$$Divergent : \Gamma_{div}(p) = \Gamma_{constant} \sqrt{\beta p}$$

Parametrization

⇔ Inspecting the detailed behavior of the integrand, we see that η converges for the criterion, $\eta[\Gamma(p)] < \infty \quad \Leftrightarrow \quad p^3 e^{-\beta p/2} \in o(\Gamma(p))$ where, o(-) denotes the Little-Landau symbol. The feasible configurations of Γ satisfying the above conditions are ::

$$Constant \quad : \quad \Gamma_{constant} = 100 MeV$$

$$Exponential \quad : \quad \Gamma_{exp}(p) = \Gamma_{constant} e^{-\beta p/8}$$

$$Lorentzian \quad : \quad \Gamma_{Lor}(p) = \Gamma_{constant} \frac{\beta p}{1+(\beta p)^2}$$

$$Divergent \quad : \quad \Gamma_{div}(p) = \Gamma_{constant} \sqrt{\beta p}$$

⇔ *Interesting to see the effects of these variations of* Γ *on* η.

Continued..η *as function of* T

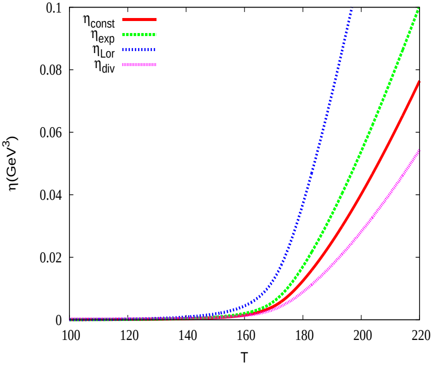

Figure: η as a function of T at vanishing chemical potential for different forms of Γ

Continued..η *as function of T*

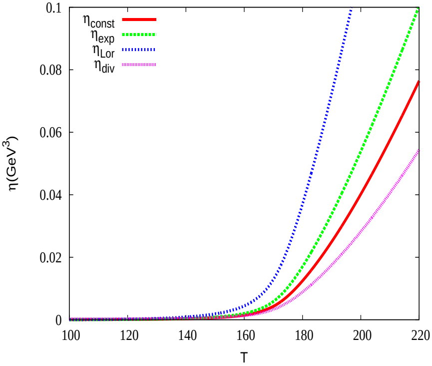

Figure: η as a function of T at vanishing chemical potential for different forms of Γ

♣ Increase of η unambiguously lessens the spectral width and vice-versa.

Continued..η *as function of* T

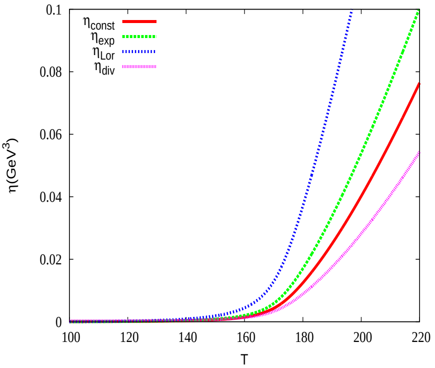

Figure: η as a function of T at vanishing chemical potential for different forms of Γ

♣ Increase of η unambiguously lessens the spectral width and vice-versa.

♣ Clearly reflected in the juxtaposition of different parametrization of Γ and hence to comprehend the nature of the figure :

Continued..η *as function of T*

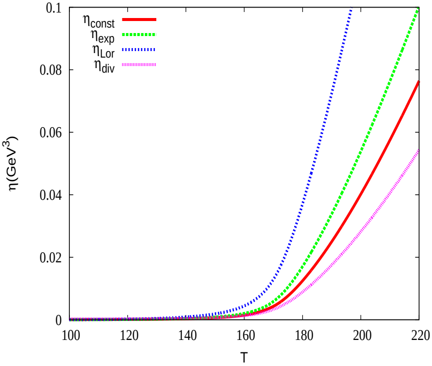

Figure: η as a function of T at vanishing chemical potential for different forms of Γ

♣ Increase of η unambiguously lessens the spectral width and vice-versa.

♣ Clearly reflected in the juxtaposition of different parametrization of Γ and hence to comprehend the nature of the figure :

$$\eta_{Lor} > \eta_{exp} > \eta_{const} > \eta_{div}$$

Continued..η *as function of* μ_q

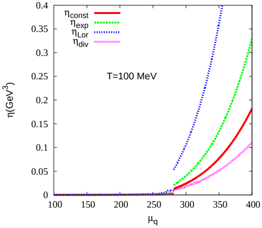

(a)

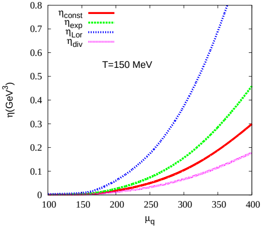

(b)

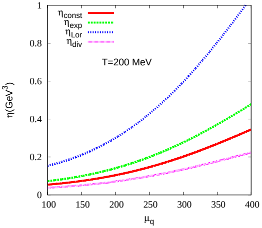

(c)

♣ The corresponding natures in the 1st order, cross-over & beyond cross-over region along the T direction meet the expectation quite well.

♣ Jump in η corresponding to T=100 MeV at around $\mu \simeq$ 280 MeV :: An issue to be discussed in the following sections.

Results :: Simulating η in detail along T & μ direction

Result I :: η *along* μ *direction*

Result I :: η along μ direction

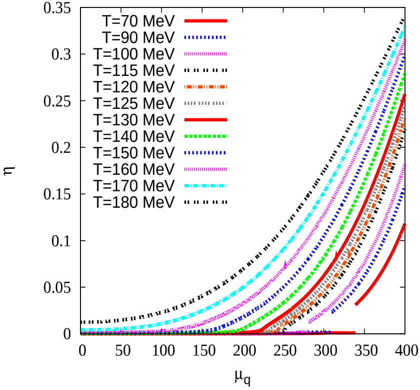

Figure: Variation of η with quark chemical potential for various T

Result I :: η along μ direction

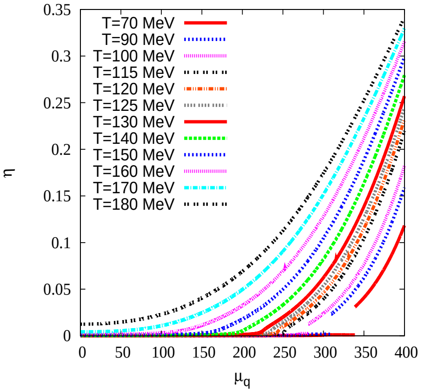

Figure: Variation of η with quark chemical potential for various T

$\Leftrightarrow$ Two distinct regimes are clearly visible.

Result I :: η along μ direction

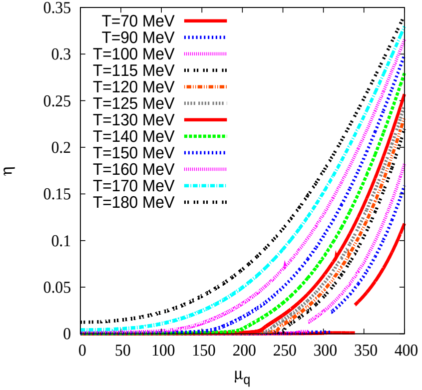

Figure: Variation of η with quark chemical potential for various T

⇔ Two distinct regimes are clearly visible.

⇔ The temperature regime of 70-100 MeV lies in the 1st order phase transition region, where η, involving 1st order pressure derivatives shows jump/discontinuity.

Result I :: η *along* μ *direction*

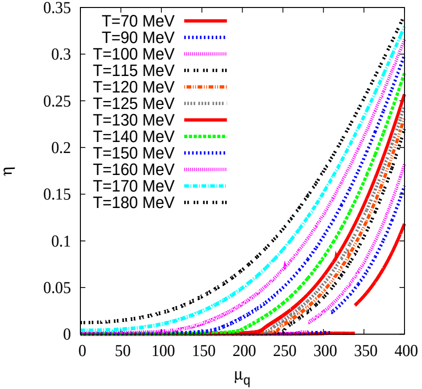

Figure: Variation of η with quark chemical potential for various T

⇔ Two distinct regimes are clearly visible.

⇔ The temperature regime of 70-100 MeV lies in the 1st order phase transition region, where η, involving 1st order pressure derivatives shows jump/discontinuity.

⇔ Whereas the T range of 120-180 MeV lies in the cross-over zone of QCD phase diagram and η expectedly shows continuous behaviour.

Result II :: $\frac{\eta}{s}$ *along* T *direction*

Result II :: $\frac{\eta}{s}$ *along* T *direction*

$\rightarrow$ Observation of minimum values of $\frac{\eta}{s}$ for different fluids.

Result II :: $\frac{\eta}{s}$ *along T direction*

$\rightarrow$ Observation of minimum values of $\frac{\eta}{s}$ for different fluids.

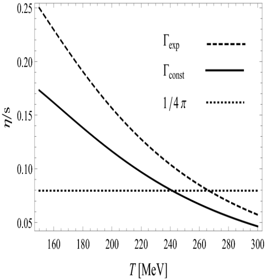

Figure: Unphysical behaviour of η/s for *constant constituent quark mass*, $M = 100 MeV$

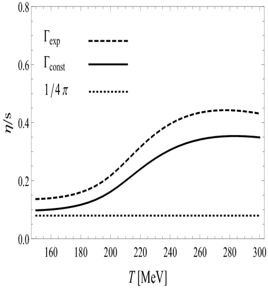

Figure: Thermal constituent quark mass, M(T,μ=0)

R.Lang, W.Weise, Eur. Phys. J. A (2014) 50 : 63

$\frac{\eta}{s}$ as function of T at vanishing μ

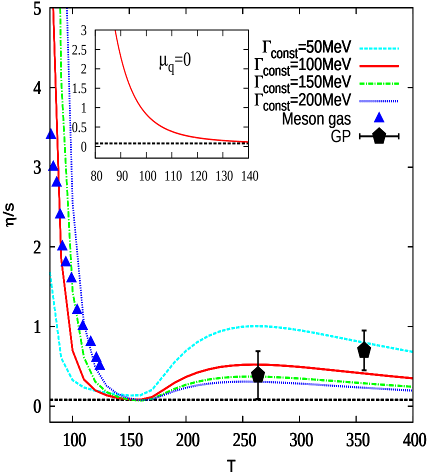

@Non-vanishing chemical potential

@Non-vanishing chemical potential

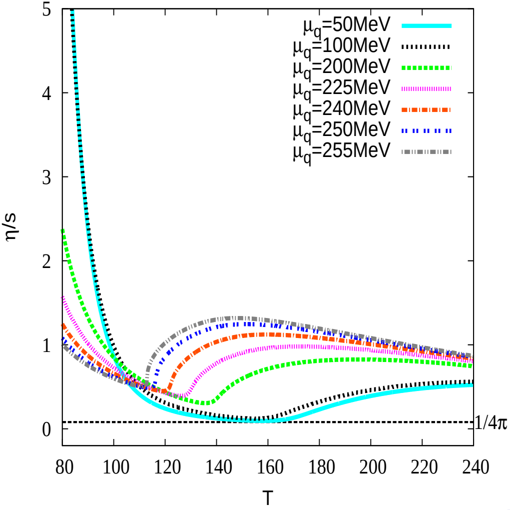

@Non-vanishing chemical potential

@Non-vanishing chemical potential

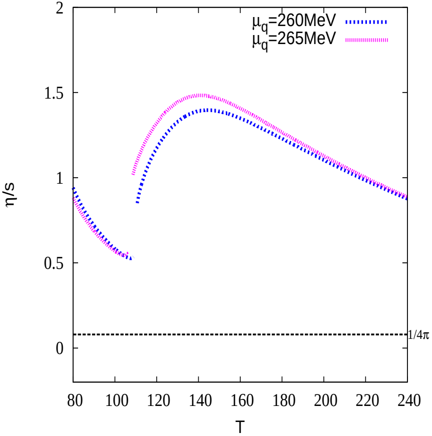

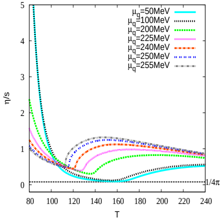

@Non-vanishing chemical potential

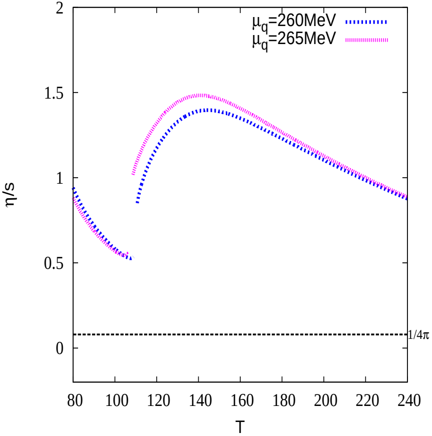

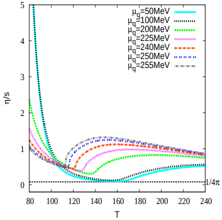

$\Leftrightarrow$ Discontinuities starting from $\mu_q \sim$ 260 MeV.

@Non-vanishing chemical potential

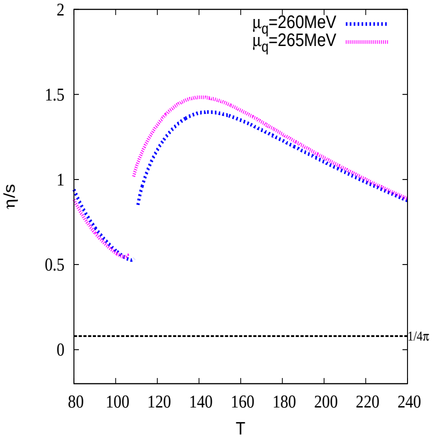

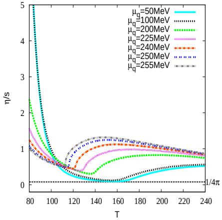

⇔ Discontinuities starting from $\mu_q \sim$ 260 MeV.
⇔ We can now draw the Phase diagram with all the tools in hand.

The Phase Diagram

The Phase Diagram

⊗ First revealed from Lattice calculations for $\mu_q = 0$ and finite T $\rightleftharpoons$ cross-over transition between Hadron gas and QGP phase.

The Phase Diagram

⊗ First revealed from Lattice calculations for $\mu_q = 0$ and finite T $\rightleftharpoons$ cross-over transition between Hadron gas and QGP phase.

⊗ Further investigations later on to indicate turning of this cross-over to a 1st order transition beyond a finite μ_q.

The Phase Diagram

$\otimes$ First revealed from Lattice calculations for $\mu_q = 0$ and finite T $\rightleftharpoons$ cross-over transition between Hadron gas and QGP phase.

$\otimes$ Further investigations later on to indicate turning of this cross-over to a 1st order transition beyond a finite μ_q.

$\otimes$ However, existence of CEP was proposed a long time before and still under bebate.

The Phase Diagram

$\otimes$ First revealed from Lattice calculations for $\mu_q = 0$ and finite T $\rightleftharpoons$ cross-over transition between Hadron gas and QGP phase.

$\otimes$ Further investigations later on to indicate turning of this cross-over to a 1st order transition beyond a finite μ_q.

$\otimes$ However, existence of CEP was proposed a long time before and still under bebate.

$\otimes$ We emphasize on the fact that at or around CEP, anomalies can occur.

The Phase Diagram

$\otimes$ First revealed from Lattice calculations for $\mu_q = 0$ and finite T $\rightleftharpoons$ cross-over transition between Hadron gas and QGP phase.

$\otimes$ Further investigations later on to indicate turning of this cross-over to a 1st order transition beyond a finite μ_q.

$\otimes$ However, existence of CEP was proposed a long time before and still under bebate.

$\otimes$ We emphasize on the fact that at or around CEP, anomalies can occur.

$\otimes$ Monitor that region where *specific shear viscosity* starts showing such behavior in terms of discontinuities.

The Phase Diagram

⊗ First revealed from Lattice calculations for $\mu_q = 0$ and finite T $\rightleftharpoons$ cross-over transition between Hadron gas and QGP phase.

⊗ Further investigations later on to indicate turning of this cross-over to a 1st order transition beyond a finite μ_q.

⊗ However, existence of CEP was proposed a long time before and still under bebate.

⊗ We emphasize on the fact that at or around CEP, anomalies can occur.

⊗ Monitor that region where *specific shear viscosity* starts showing such behavior in terms of discontinuities.

⊗ As was argued previously minimum of $\frac{\eta}{s}$ occur near phase transition, we locate μ_q^C, T^C.

The Phase Diagram

⊗ First revealed from Lattice calculations for $\mu_q = 0$ and finite T $\rightleftharpoons$ cross-over transition between Hadron gas and QGP phase.

⊗ Further investigations later on to indicate turning of this cross-over to a 1st order transition beyond a finite μ_q.

⊗ However, existence of CEP was proposed a long time before and still under bebate.

⊗ We emphasize on the fact that at or around CEP, anomalies can occur.

⊗ Monitor that region where *specific shear viscosity* starts showing such behavior in terms of discontinuities.

⊗ As was argued previously minimum of $\frac{\eta}{s}$ occur near phase transition, we locate μ_q^C, T^C.

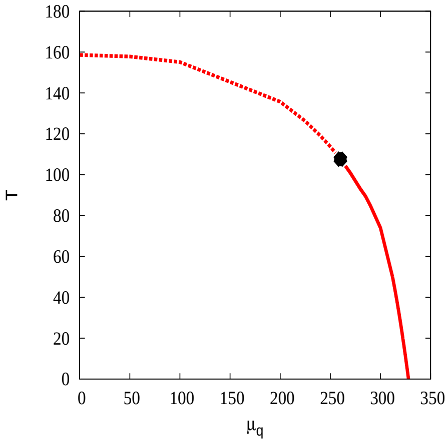

On The location of CEP..

On The location of CEP..

$$\mathbf{C_V} = \frac{\partial \epsilon}{\partial \mathbf{T}} = \mathbf{T}\frac{\partial^2 \mathbf{P}}{\partial \mathbf{T}^2} = \mathbf{T}\frac{\partial \mathbf{s}}{\partial \mathbf{T}}$$

$\Leftrightarrow$ A transition parameter which can show distinguishable nature near CEP, noticeably a 2nd order transition region.

On The location of CEP..

$$\mathbf{C_V} = \frac{\partial\epsilon}{\partial \mathbf{T}} = \mathbf{T}\frac{\partial^2 \mathbf{P}}{\partial \mathbf{T}^2} = \mathbf{T}\frac{\partial \mathbf{s}}{\partial \mathbf{T}}$$

⇔ A transition parameter which can show distinguishable nature near CEP, noticeably a 2nd order transition region.

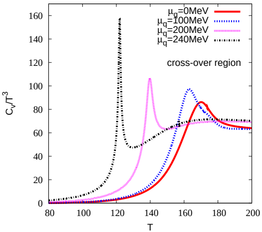

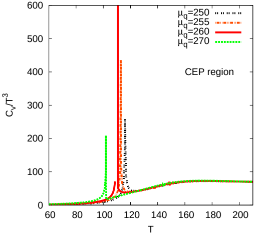

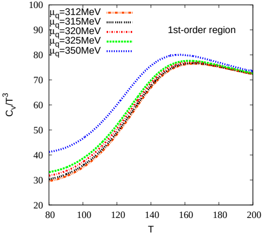

♣ C_V **being a 2nd order derivative of pressure , shoots up in the regime of** $\mu_q \sim 260$ **MeV, otherwise shows continuous behaviour**.

Connection with experiments

[3] F. Karsch and K. Redlich, PLB 695, 136 (2011)

Connection with experiments

♣ The independent parameters in our case :: $T,\ \mu_B,\ \mu_Q,\ \mu_S$.

[3] F. Karsch and K. Redlich, PLB 695, 136 (2011)

Connection with experiments

- The independent parameters in our case :: $T,\ \mu_B,\ \mu_Q,\ \mu_S$.
- Freeze-out parametrization by Redlich *et. al*. has been used [3]

$$T(\mu_B) = a - b\mu_B^2 - c\mu_B^4$$
$$\mu_{B,Q,S}(\sqrt{s}) = \frac{d}{1+e\sqrt{s}}$$

	$d[GeV]$	$e[GeV^{-1}]$
B	1.308(28)	0.273(8)
Q	0.0211	0.106
S	0.214	0.161

where, $a = (0.166 \pm 0.002)GeV$, $b = (0.139 \pm 0.016)GeV^{-1}$, $c = (0.053 \pm 0.021)GeV^{-3}$

[3] F. Karsch and K. Redlich, PLB 695, 136 (2011)

Connection with experiments

- The independent parameters in our case :: $T, \ \mu_B, \ \mu_Q, \ \mu_S$.
- Freeze-out parametrization by Redlich *et. al.* has been used [3]

$$T(\mu_B) = a - b\mu_B^2 - c\mu_B^4$$
$$\mu_{B,Q,S}(\sqrt{s}) = \frac{d}{1+e\sqrt{s}}$$

	$d[GeV]$	$e[GeV^{-1}]$
B	1.308(28)	0.273(8)
Q	0.0211	0.106
S	0.214	0.161

where, $a = (0.166 \pm 0.002)GeV, \ \ b = (0.139 \pm 0.016)GeV^{-1}, c = (0.053 \pm 0.021)GeV^{-3}$

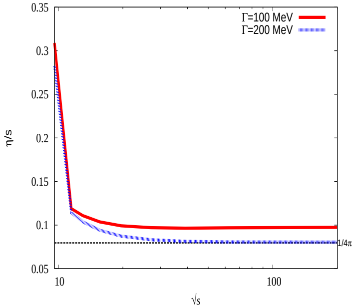

[3] F. Karsch and K. Redlich, PLB 695, 136 (2011)

Conclusions

Conclusions

- Inclusion of non-idealities like viscous effects is very essential in order to get a flavor of degree of perfectness of the fluid under concern.

Conclusions

- Inclusion of non-idealities like viscous effects is very essential in order to get a flavor of degree of perfectness of the fluid under concern.

- Various regions of the phase diagram are expected to be arrested through phenomenological studies.

Conclusions

- Inclusion of non-idealities like viscous effects is very essential in order to get a flavor of degree of perfectness of the fluid under concern.

- Various regions of the phase diagram are expected to be arrested through phenomenological studies.

- We presented justifications through computation of appropriate variables to reconfirm the location of CEP.

Conclusions

- Inclusion of non-idealities like viscous effects is very essential in order to get a flavor of degree of perfectness of the fluid under concern.

- Various regions of the phase diagram are expected to be arrested through phenomenological studies.

- We presented justifications through computation of appropriate variables to reconfirm the location of CEP.

- All the facts and arguments strengthen the validity of the technique we used to draw the phase diagram.

Conclusions

- Inclusion of non-idealities like viscous effects is very essential in order to get a flavor of degree of perfectness of the fluid under concern.

- Various regions of the phase diagram are expected to be arrested through phenomenological studies.

- We presented justifications through computation of appropriate variables to reconfirm the location of CEP.

- All the facts and arguments strengthen the validity of the technique we used to draw the phase diagram.

- Experimental studies indicate towards very small specific shear viscosity for QGP phase which is similar to what we get in our findings.

Collaborators

- Kinkar Saha
- Dr. Rajarshi Ray
- Prof. Sanjay K. Ghosh
- Prof. Abhijit Bhattacharyya
- Prof. Sibaji Raha
- Dr. Supriya Das


Thank you